Nonequilibrium relaxation analysis of a quasi-one-dimensional frustrated *XY* model for charge-density waves in ring-shaped crystals

Tomoaki Nogawa* and Koji Nemoto†
Division of Physics, Hokkaido University, Sapporo, Hokkaido 060-0810, Japan
(Received 15 November 2005; revised manuscript received 1 February 2006; published 2 May 2006)

We propose a model for charge-density waves in ring-shaped crystals, which depicts frustration between intra- and interchain couplings coming from cylindrical bending. It is then mapped to a three-dimensional uniformly frustrated *XY* model with one-dimensional anisotropy in connectivity. The nonequilibrium relaxation dynamics is investigated by Monte Carlo simulations to find a phase transition which is quite different from that of usual whisker crystal. We also find that the low-temperature state is a three-dimensional phase vortex lattice with a two-dimensional phase coherence in a cylindrical shell and the system shows power-law relaxation in the ordered phase.

DOI: 10.1103/PhysRevB.73.184504 PACS number(s): 74.25.Dw, 71.45.Lr, 64.60.Ht, 05.10.Ln

I. INTRODUCTION

Transition-metal chalcogenides such as $NbSe_3$ and TaS_3 are known as quasi-one-dimensional materials. Lowering temperature, they take a phase transition to the charge-density wave (CDW) phase where both the atom positions and electronic charge density are modulated in twice the Fermi wave number.[1] Recently, Tanda and Tsuneta *et al.* have succeeded to synthesize various types of single crystals in closed loop shapes, e.g., simple ring, Möbius ring, and figure-of-eight, of these materials by the chemical vapor transportation method.[2,3] X-ray diffraction measurement shows that they have the same crystalline structure with usual whisker crystals and the temperature dependence of conductivity indicates a CDW transition at the temperature slightly lower than the critical temperature of whisker crystals.[4] The influence of the crystal geometry or topology on the property is an interesting problem.

Recently, Shimatake and Toda investigated nonequilibrium relaxation dynamics of $NbSe_3$ by using ultrafast laser.[5] They measured both ring and whisker crystals with comparable dimensions and found a significant difference between them in the low-temperature CDW phase. The relaxation time for the initial rapid decay shows divergent behavior at the transition temperature for a whisker crystal but not for a ring crystal. This suggests that the phase transition disappears or the type of phase transition changes for ring crystals. In this paper, we propose a simple model for CDWs in ring crystals and analyze the nonequilibrium relaxation dynamics by the Monte Carlo method to understand the reason for such a difference.

II. MODEL FOR CDW IN RING CRYSTAL

At first, we introduce a phase field model for CDW in a ring crystal. The crystal axes are named *a*, *b*, and *c* axes as illustrated in Fig. 1. The quasi-one-dimensional chains run along the *b* axis. The position in a sample is expressed as $\mathbf{r}=(x_a,x_b,x_c)=(r,r\phi,x_c)$ by using cylindrical coordinates. The modulated part of the charge density can be expressed as $\rho(\mathbf{r},t)=\rho_0\cos[Q(r)x_b+\theta(\mathbf{r},t)]$ in each chain. Here, $Q(r)$ is the mean wave number of a chain at radius r and $\theta(\mathbf{r},t)$ is the phase fluctuation variable. Periodic boundary condition along a chain yields $Q(r)2\pi r=2\pi N_w(r)$, where $N_w(r)$ is a number of waves in a chain. $Q(r)$ possibly deviates from the natural wave number of CDW, $Q_0=2k_F$, to synchronize the charge-density modulations between neighboring chains. Such commensuration between the chains neighboring on the radial direction results in strain. The stress grows with the thickness and is released by making some imperfection, such as a jump of N_w, by every several chains. We consider that the characteristic relaxation dynamics of a ring crystal is due to such conflict between two requirements for the natural wavelength inside each chain and for period matching between neighboring chains.

Here we suppose bundles of looped chains in which no defect exists and then $N_w(r)$ is constant. The mean wave number decreases with radius as $Q(r)=N_w/r$ in each bundle. The wave number is larger than the natural one for inner edges and smaller for outer edges. The Coulomb interaction V_α at the boundary of two neighboring bundles is proportional to the product of charge densities as

$$V_a \propto \int dx_b \cos[Q_\downarrow x_b+\theta_\downarrow(x_b)]\cos[Q_\uparrow x_b+\theta_\uparrow(x_b)]$$
$$=\frac{1}{2}\int dx_b\{\cos[\theta_\downarrow(x_b)-\theta_\uparrow(x_b)-\Delta Q x_b]$$
$$+\cos[\theta_\downarrow(x_b)+\theta_\uparrow(x_b)+(Q_\downarrow+Q_\uparrow)x_b]\}. \quad (1)$$

The down- (↓) and up- (↑) arrows indicate quantities of the inner and outer bundles, respectively. $\Delta Q(r)\equiv Q_\uparrow-Q_\downarrow$ is a

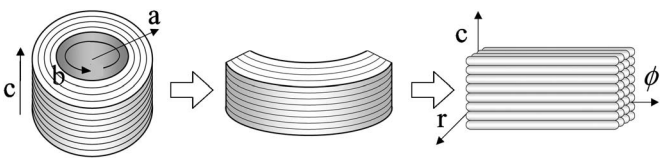

FIG. 1. Schematic diagram of ring crystal and mapping onto cuboid.

gap of wave number at the boundary between the two neighboring bundles. In this expression, we keep track of the first term only and neglect the second term because it oscillates much faster than $\theta(x_b)$ changes.

Knowing the above interaction form between the phases $\theta_\uparrow$ and $\theta_\downarrow$, let us consider a discrete version of the phase Hamiltonian. We map the ring crystal onto a simple cubic lattice with size $N=L_a\times L_\phi\times L_c$ (see Fig. 1). Note that the space is divided uniformly in ϕ instead of $x_b=r\phi$. The lattice spacings are taken as a mesoscopic scale, much larger than the CDW wavelength. Adding intrachain distortion energy and interbundle energy on the c axis to Eq. (1), the Hamiltonian is written as

$$H=-\sum_{\alpha=a,b,c}\sum_{\mathbf{i}} J_\alpha \cos(\theta_{\mathbf{i}}-\theta_{\mathbf{i}+\hat{\alpha}}-A_{\mathbf{i},\mathbf{i}+\hat{\alpha}}). \tag{2}$$

Here, $\mathbf{i}$ labels the lattice points of a simple cubic lattice and $\hat{\alpha}$ is the unit lattice vector on the α axis. What is important is that there is an additional term,

$$A_{\mathbf{i},\mathbf{i}+\hat{\alpha}}\equiv \Delta Q x_b \delta_{\alpha a}=\Delta N_w \phi \delta_{\alpha a}=2\pi f i_b \delta_{\alpha a}, \tag{3}$$

which comes from the ring geometry. $\Delta N_w=r\Delta Q$ is a gap of a number of waves and $f=\Delta N_w/L_\phi$ is a filling factor that denotes the mean density of vortices. A_{ij} causes a frustration between the couplings along a and b axes and yields a constant number of phase vortex lines directed to the c axis even without thermal excitation. The vorticity is given by the loop integration of $\nabla\theta$ along each plaquette. By omitting $A_{\mathbf{ij}}$, we obtain a usual XY model, which is applicable to CDWs in whisker crystals.

The Hamiltonian Eq. (2) is equivalent to the uniformly frustrated XY model, which is proposed for the superconductors under magnetic field parallel to the c axis,[6–8] where A_{ij} is translated to a vector potential in the Landau gauge. The anisotropy is, however, quite different. While the high-T_c superconductor has strong coupling inside each CuO_2 plane and weak one interplanes, CDW materials has quasi-one-dimensional property. The anisotropy in coupling constants is taken as $J_b=\gamma J_a=\gamma J_c$, $\gamma>1$ in the present model. Since the distance between lattice points neighboring on the b axis is proportional to r, coupling constants and filling factor should depend on the radius r, but we ignore this r dependence as a first approximation.

At first, we investigate the ground state of this Hamiltonian. By simulated annealing, we obtained an energy minimal state for sufficiently large γ. This state has ΔN_w phase vortex lines between every neighboring bc plane, which are straight and parallel to the c axis. These vortex lines form a two-dimensional lattice in the ab plane with the unit lattice vectors $(\pm a_0, b_0/2f, 0)$. Order parameter r_v, which is related to the Bragg peak height of a vortex lattice, can be defined as follows:

$$r_v=S_v(\mathbf{q}_v)/N,\quad \mathbf{q}_v=(2\pi/2a_0, 2\pi f/b_0, 0),$$

$$S_v(\mathbf{q})=N^{-1}\langle |v_c(\mathbf{q})|^2\rangle,$$

$$v_c(\mathbf{q})=\sum_{\mathbf{j}}(\mathbf{v_j}\cdot\hat{\mathbf{c}})\exp(i\mathbf{q}\cdot\mathbf{r_j}). \tag{4}$$

Here $(\mathbf{v_j}\cdot\hat{\mathbf{c}})$ is the vorticity defined at the center of a plaquette $\mathbf{j}$ which is perpendicular to the c axis. Owing to the strong coupling along the b axis, the phase is almost uniform along the direction but gently modulated with a period b_0/f. This state looks quite different from the solitonic solution in the isotropic case where distortion is localized around the vortex. Simple variational calculation supposing the periods $2a_0$ and b_0/f along a and b axes, respectively, yields an energy minimal solution expressed as

$$\theta_{\mathbf{i}}=(-1)^{i_a}\left[\frac{\pi}{4}-\frac{2\gamma^{-1}}{(2\pi f)^2}\cos(2\pi f i_b)\right]+O(\gamma^{-2}), \tag{5}$$

which agrees well with the simulated annealing result. Note that there are many energetically degenerated states which are obtained by the transformation $\theta_{\mathbf{i}}\rightarrow\theta_{\mathbf{i}}+2\pi n i_a/L_a$ ($n=\pm1,\pm2,\ldots$). This transformation does not change the positions of vortices.

III. NONEQUILIBRIUM RELAXATION ANALYSIS OF PHASE TRANSITION

Next we investigate the relaxation dynamics from an ordered state to an equilibrium state at finite temperature, i.e., a rapid heating process. At the same time, the phase transition is also analyzed by the nonequilibrium relaxation method.[9] In order to obtain an initial state, we set the phases as Eq. (5) and make the system relax at zero temperature in diffusive dynamics. After that, METROPOLIS dynamics at finite temperature is started. Filling factor f is fixed to $1/16$ in this work. The same calculation is done for several anisotropy parameters, $\gamma=10$, 16, 24, 32, and 64. The Monte Carlo flip is repeated up to 65 000 steps per each site at maximum. This step is identified as time, t. Average is taken over 8–16 samples for each temperature. The sample size used is $L_a\times L_\phi\times L_c=64\times512\times64$ and periodic boundary condition is imposed for all directions. For this system size, the finite-size effect is not crucial within the observation time.

The order parameter r_v equals f^2 in the initial state and decreases to the equilibrium value which is zero when $T\geqslant T_c$ and finite when $T<T_c$. To find the critical point, we calculate the local exponent,[9]

$$\lambda(t)=-d\ln r_v(t)/d\ln t. \tag{6}$$

In Fig. 2, $\lambda(t)$ is plotted with respect to $1/t$. In the limit of $t\rightarrow\infty$, $\lambda(t)$ goes to infinity for $T>T_c$ and to zero for $T<T_c$. Just at the critical temperature, $\lambda(t)$ converges to a certain finite exponent λ_c which characterizes the critical power-law decay.

For $T>T_c$, r_v decays as a power function of t for short time scale and makes a crossover to exponential decay. We can perform dynamical scaling as

$$r_v(t)=\tau(T)^{-\lambda_c}\tilde{S}_v[t/\tau(T)]. \tag{7}$$

Here $\tau(T)$ is a relaxation time, which diverges at the critical temperature T_c as

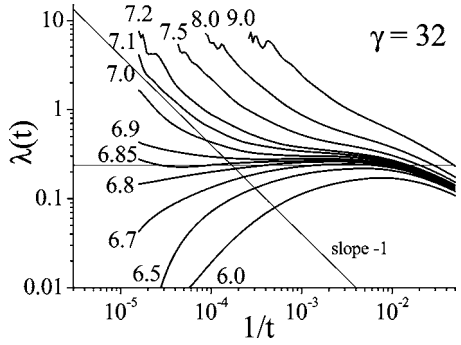

FIG. 2. The local exponent of the order parameter r_v for various temperatures, as a function of $1/t$. The temperature of each curve is shown in the figure in the unit of J_a/k_B (T_c=6.87J_a/k_B). The derivative is calculated after local fitting to a fourth-order polynomial. The anisotropy parameter γ equals 32. The horizontal line shows λ_c obtained by dynamical scaling.

$$\tau(T) \propto (T/T_c - 1)^{-z\nu}. \tag{8}$$

We initially obtain λ_c and $\tau(T)$'s by scaling to Eq. (7). Then fitting of $\tau(T)$'s to Eq. (8) yields T_c and $z\nu$. The scaling result for γ=32 is shown in Fig. 3. The results for several γ's are summarized in Table I. T_c is proportional to $(J_bJ_c)^{1/2}$, which measures the effective elasticity of vortex lines confined between two bc planes. The exponent λ_c seems not universal among different γ's. It shows, however, a sign for saturation to the anisotropic limit value $\approx$0.25 as γ becomes large. $z\nu$ is less dependent of γ even for small γ.

For small γ, dynamical scaling does not work well *in the very vicinity of* the critical temperature, where the functional form of relaxation changes with temperature. In Fig. 4, the local exponent for γ=10 is plotted with $1/t$. If the relaxation form is a simple exponential one in the long-time limit, $\lambda(t)$ would be asymptotically proportional to t. Figure 4 shows, however, $\lambda(t) \propto t^{\mu}$, where μ is larger than unity and increases up to 2 as approaching the critical temperature. Such a bad scaling region in temperature, however, becomes narrower as γ increases.

IV. RELAXATION DYNAMICS IN THE ORDERED PHASE

Next, we investigate the relaxation function in the low-temperature phase. In order to eliminate the influence of the finite equilibrium value, the time derivative of the order parameter is calculated. The relaxation of r_v does not look like an exponential function in the time range of the present simulations. We do not find an apparent reduction of relaxation time when leaving from the critical point unlike in the high-temperature phase. Although the functional form of r_v is unclear, the power-law behavior is observed to be suitable for some other quantities, e.g., total energy of the system and the order parameter of phase periodicity r_θ^b. Here

TABLE I. Critical temperature in the unit of $(J_bJ_c)^{1/2}/k_B$ and exponents for several anisotropy parameters. LE means the critical temperature is estimated from the long-time behavior of local exponent and DS means dynamical scaling.

γ	T_c (LE)	T_c (DS)	λ (DS)	$z\nu$ (DS)
10	1.159(2)	1.13	0.06	2.2
16	1.190(5)	1.17	0.16	2.1
24	1.208(6)	1.18	0.22	2.2
32	1.214(5)	1.20	0.24	2.2
64	1.206(6)	1.18	0.25	2.6

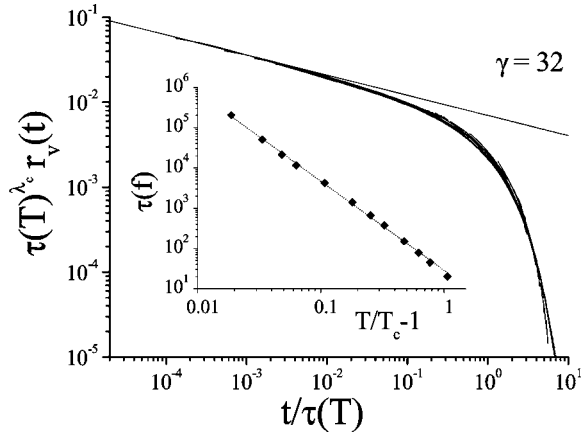

FIG. 3. Scaling plot for γ=32. The temperatures for used data are 6.9, 7.0, 7.1, 7.2, 7.5, 8.0, 8.5, 9.0, 10.0, 11.0, 12.0, and 14.0J_a/k_B. The inset shows critical behavior of the relaxation time.

$$r_\theta^b \equiv S_\theta(\mathbf{q}_\theta^b)/N. \tag{9}$$

Here $S_\theta(\mathbf{q})$ is a Fourier transformation of phase correlation function defined as

$$S_\theta(\mathbf{q}) = N^{-1}\sum_{\mathbf{i},\mathbf{j}} \cos(\theta_\mathbf{i} - \theta_\mathbf{j})\exp[i\mathbf{q}\cdot(\mathbf{r_i} - \mathbf{r_j})], \tag{10}$$

which has peaks at $\mathbf{q}_\theta^a \equiv (2\pi/a_0, 0, 0)$ and $\mathbf{q}_\theta^b \equiv (0, 2\pi f/b_0, 0)$. Note that this order parameter is finite at t=0 only because the initial state is chosen as Eq. (5) and other metastable states have peaks in different wave-number vectors. The time evolution of r_θ^b and tdr_θ^b/dt is shown in Fig. 5. For $T<T_c$, r_θ^b seems to decay to a finite value in the limit of $t\to\infty$. This indicates that not only the vortex but also the phase has true long-range periodic order in three dimensions.

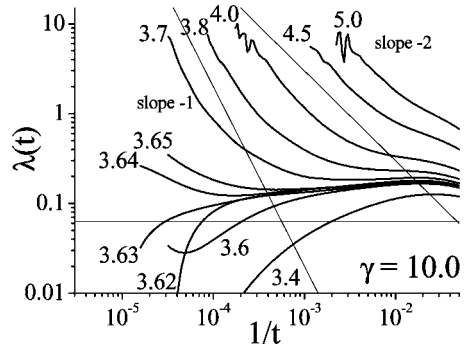

FIG. 4. The local exponent for a relatively small anisotropic parameter γ=10.

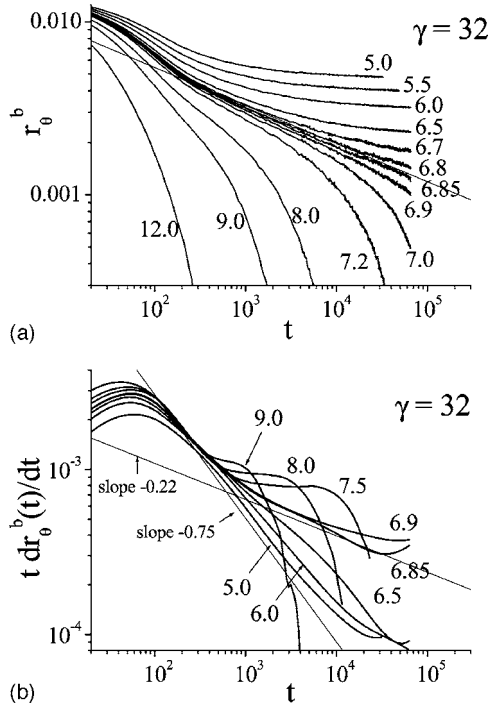

FIG. 5. Time evolution of phase structure factor r_θ^b (top) and time derivative of r_θ^b *multiplied by* t (bottom). The derivative is obtained by local fitting to a fourth-order cubic polynomial. The line of slope −0.22 means the relaxation at the critical temperature.

We confirm that this finite value does not come from the finite-size effect. The time derivative shows power-law relaxation with t. The decay exponent becomes larger with T.

V. DISCUSSION

A. Dimensionality of periodic order

So far, it has been shown that the quasi-one-dimensional frustrated XY model takes a vortex lattice melting transition. The dynamical scaling analysis strongly suggests that it is a standard second-order transition. Then r_v and r_θ^b work as order parameters of vortex and phase itself.

By equilibrium simulations, we find that the helicity modulus, which measures the thermodynamic stiffness of phase against the perturbation, $\theta_{\mathbf{i}} \to \theta_{\mathbf{i}} + \epsilon i_\alpha (\epsilon \to 0)$,[6] is zero along the a axis for all temperatures while those along b and c axes are finite below T_c. This means that the (quasi)-long-range phase coherence is established only in the ab plane.

The reason why the two-dimensional phase coherence appears in a quasi-one-dimensional system is considered as follows: Even with $J_a = J_c (\ll J_b)$, the a and c axes are not equivalent since the former conflicts with the b axis and the latter does not. The fast growth of the order along the b axis suppresses the order along the a axis; two-dimensional-like order then appears.

Power-law behavior and two-dimensional order remind us of the Kosterlitz-Thouless (KT) phase[10] with quasi-long-range order. If so, it is strange that r_θ^b is finite in the long-time limit as shown in the previous section. Furthermore, finite r_θ^b seems directly inconsistent with the fact that the helicity modulus for the a axis is zero. Of course we cannot eliminate the possibility that r_θ^b decreases to zero in the time scale much longer than the present observation time, but there can be another explanation, as follows. When the two-dimensional *true* long-range order is established, the center of mass of its phase is individually pinned in every bc- plane due to the break of ergodicity. As a result, the phase fluctuation along the a axis is suppressed even though there is no restoring force. Thus finite r_v, which is due to the initial condition, survives even though long-range order exists only in two dimensions. In contrast, vorticity is a gauge invariant quantity and really has three-dimensional long-range order. If this is true, there would be another mechanism for the power decay which differs from the KT scenario, on which r_θ^b goes to zero. Indeed, power divergence of relaxation time at T_c is inconsistent with the exponential divergence for the KT transition.[9]

B. Comparison with in-plane isotropic case

Here we compare the present result with high-T_c superconductors. The case of the magnetic field perpendicular to the CuO_2 plane is given by $J_a = J_b \gg J_c$ in the present notation. This is isotropic in the frustrated ab plane. It is believed that there is a first-order transition[8] into the low-temperature phase where phase coherence exists only along the c axis.[7] The limit $\gamma \to 1$ in the present model is also expected to show the same transition, although the discontinuous property is quite small in the case in which J_c is as large as J_a, J_b.[7] There is a possibility that bad scaling behavior near T_c for smaller γ as mentioned at the last of Sec. III is due to the crossover to a first-order transition.

Power-law relaxation is also observed in the isotropic frustration model.[6] This is apparently unrelated to the KT order. We consider that the power-law behaviors of the isotropic and anisotropic models are a common property of the partially ordered states of frustrated systems, although dimensionality of phase ordering is different.

C. Comparison with the quasi-two-dimensional case

The case of a magnetic field parallel to the CuO_2 plane can be expressed by the present model with $\gamma \ll 1$, although the CuO_2 plane is normal to the b axis, not to the c axis.[13] This is just the opposite anisotropy to the present study and the system is divided into isolated planes without frustration in the strong anisotropy limit. This case, however, has many common properties with the present case of $\gamma \gg 1$ in spite of the difference in quasi-two- and one-dimensional properties, e.g., two-dimensional phase coherence parallel to the c axis and the same structure of vortex lattices.[11,12] Additionally the phase transitions change from first order to second order as anisotropy becomes stronger in both cases. This similarity comes from the fact that qualititative behavior is not affected by the strength of the coupling along the c axis, which is not concerned with the frustration of the system. It is essential that both of these opposite anisotropies, $\gamma \gg 1$ and $\gamma \ll 1$, break the balance of frustration in the ab plane in the same way.

The vortex lattice order in the quasi-two-dimensional system is considered to be of quasi-long-range.[12] It is also reported that the two-layer system (this is purely two dimensional) has two types of KT phases,[14,15] the vortex phase and the Meissner phase. It is, however, not clear whether the interlayer coupling in three-dimensional system could be irrelevant for small but finite γ. We consider that true long-range order assisted by three-dimensional vortex lattice order is worth reexamining in the quasi-two-dimensional case as well as the present case.

D. Experiment

Finally, let us mention about the relation to the experiments of a CDW in a ring crystal.[5] The present work based on the anisotropic frustrated *XY* model found a phase transition to the ordered state where phase vortex lines along the *c* axis form a lattice and two-dimensional phase coherence is established in each cylindrical shell perpendicular to the radius direction. Thus it suggests that the ring geometry makes the CDW phase transition quite different from that of a whisker crystal. The latter is described by the *XY* model without frustration, which shows a simple ferromagnetic transition. In the low-temperature phase of a ring crystal, the relaxation of phase fluctuation, which is closely connected to electric polarization and reflectivity, shows a power-law relaxation without characteristic time scale, so that small apparent relaxation time, which does not show singular behavior, would be estimated if one supposes an exponential decay as for whisker crystals.

There remain some future works. In this work, the rapid heating process is studied because of its self-averaging property instead of rapid cooling process. The latter is challenging because it can be compared directly with the laser pumping experiment and contains the process to untwist entangled flux lines. The present model drops some features of the system, e.g., radius dependence of the model parameters, which causes distribution of local critical temperature and relaxation time (the transition can then be blurred) and a pinning effect of lattice defects in atomic crystal.

ACKNOWLEDGMENTS

The authors thank S. Tanda, Y. Toda, and K. Shimatake for useful discussions. This work is supported by 21st Century COE program "Topological Science and Technology."

*Electronic address: nogawa@statphys.sci.hokudai.ac.jp
†Electronic address: nemoto@statphys.sci.hokudai.ac.jp

[1] G. Grüner, Rev. Mod. Phys. **60**, 1129 (1988).
[2] S. Tanda, T. Tsuneta, Y. Okajima, K. Inagaki, K. Yamaya, and N. Hatakenaka, Nature (London) **417**, 397 (2002).
[3] T. Tsuneta and S. Tanda, J. Cryst. Growth **264**, 223 (2004).
[4] S. Tsuneta, S. Tanda, Y. Okajima, K. Inagaki, and K. Yamaya, Physica B **329**, 1544 (2003).
[5] K. Shimatake, Y. Toda, and S. Tanda, Phys. Rev. B **73**, 153403 (2006).
[6] Y. H. Li and S. Teitel, Phys. Rev. B **47**, 359 (1993).
[7] T. Chen and S. Teitel, Phys. Rev. B **55**, 11766 (1997).
[8] X. Hu, S. Miyashita, and M. Tachiki, Phys. Rev. Lett. **79**, 3498 (1997).
[9] Y. Ozeki, K. Ogawa, and N. Ito, Phys. Rev. E **67**, 026702 (2003).
[10] J. M. Kosterlitz and D. J. Thouless, J. Phys. C **6**, 1181 (1973).
[11] X. Hu and M. Tachiki, Phys. Rev. Lett. **85**, 2577 (2000).
[12] X. Hu and M. Tachiki, Phys. Rev. B **70**, 064506 (2004).
[13] L. Balents and D. R. Nelson, Phys. Rev. Lett. **73**, 2618 (1994).
[14] E. Orignac and T. Giamarchi, Phys. Rev. B **64**, 144515 (2001).
[15] E. Granato, Phys. Rev. B **72**, 104521 (2005).